Effect of Temperature on Polyethylene Teraphthalate Coated ECCS Plates in Acetic-Acetate Medium

E. Zumelzu,[1] F. Rull,[2] C. Ortega,[3] C. Cabezas[4]

[1]*Instituto de Materiales y Procesos Termomecanicos, Universidad Austral de Chile, Valdivia, Chile*
[2]*Dpto. Física de la Materia Condensada, Universidad de Valladolid, Spain*
[3]*Escuela de Mecánica, Facultad de Ciencias de Ingeniería, Universidad Austral de Chile, Valdivia, Chile*
[4]*Instituto de Química, Universidad Austral de Chile, Valdivia, Chile*

Received 3 September 2008; accepted 19 January 2009
DOI 10.1002/app.30077
Published online 17 April 2009 in Wiley InterScience (www.interscience.wiley.com).

ABSTRACT: Electrolytic chromium-coated steel plates with a polyethylene teraphthalate (PET) polymer coating, used in the manufacturing of both flat and rippled wall cans and containers, were submitted to 40, 60, and 80°C heating in an acetic-acetate medium and to electrochemical polarization tests, to study the PET coating degradation and the structural changes leading to a loss of the protection capacity of the steel, as well as to determine the detachment at the interface level. The samples were analyzed by Raman vibrational spectroscopy, micro-Raman, and attenuated total reflection to evaluate changes in the composition and structure of the coatings. Also, the PET surface was characterized by scanning electron microscopy (SEM) to establish the coating degradation. Spectroscopy analyses showed small changes of crystallinity in the PET thickness at 80°C and a reduced effect of the mechanical forming of plates on crystallinity. The SEM characterization evidenced the presence of surface defects and failures on the coating caused by the acetic-acetate medium. © 2009 Wiley Periodicals, Inc. J Appl Polym Sci 113: 1853–1859, 2009

Key words: steel; coating; degradation; acetic-acetate; characterization; spectroscopy

INTRODUCTION

The metal-polymers plates are intended to replace the conventional steel containers coated with sanitary lacquers, because of the minimum emission of solvents and chemical elements when compared with the traditional lacquers.

In this sense, the electrolytic chromium-coated steels (ECCS), surface-protected by a polyethylene teraphthalate (PET) co-rolled layer, are multifunctional advanced materials that incorporate an improved protection-barrier effect and are more environmental-friendly in their manufacturing processes.

PET coatings have unique properties, which provide waterproof protection to the ECCS plates, prevent physicochemical interactions with the environment, and offer resistance to surface mechanical damages during handling and transport of the metal sheets.[1]

The polymer-coated sheets can undergo damage during rolling and forming resulting in fracture, detachment of the polymer layer, discontinuities between coating and substrates, and the presence of surface microdeformations after these processes.[2,3] All of these features are of considerable importance to determine the formability limits of this multilayer material.

The PET layer can be subject to thermomechanical deformation during the processing and manufacturing of plates, such as extrusion, drawing, and molding. It is important to highlight that during these processes, microstructural ,and mechanical properties of PET coatings are for the most part independent.

Recently, other studies including spectroscopy observations, calorimetric measurements, and X-ray scattering methods have shown that a three-phase model is more appropriate to describe the PET microstructure. This model states that the amorphous phase of the PET consists of two fractions: the true or mobile amorphous fraction and the rigid amorphous fraction that holds a partial order, and which is positioned between the mobile amorphous fraction and the crystalline.[4,5]

In the authors' studies, an intermediate phase with regard to the amorphous and crystalline stages, and close to the metal interface, was found by ultrathin slices of 300 Å and transmission electron microscopy observations of PET-coated ECCS plates.[6,7] There are discrepancies about the most suitable structural

Correspondence to: E. Zumelzu (ezumelzu@uach.cl).
Contract grant sponsor: Fondecyt Projects; contract grant numbers: 1070375, 7070062.
Contract grant sponsor: Universidad Austral de Chile.

model concerning its properties, such as permeability to oxygen,[8] mechanical behavior, heating capacity, and complex behaviors when bound to diverse polymers such as PET.[9,10] The employment of PET on a steel sheet, creating a metal-polymer composite, hinders the understanding of the deformation behavior to deformation of the different substrates.

In other recent works, the effect of the acetic-acetate medium, representative of the action of foods like fish and shellfish, on PET-coated ECCS containers has been studied by means of immersion vs. time trials at room temperature. It was possible to determine that after nine months of exposure the PET suffered significant degradation by the medium, limiting the protection capacity of the coating and its useful life in containers.

This study is aimed at evaluating under controlled experimental conditions the effect of temperature on PET-coated ECCS plates in an acetic-acetate medium, simulating the thermal shock conditions occurring during food canning. A later evaluation of the system through electrochemical polarization of the samples, allows as a whole the determination of the occurrence of PET degradation by evidencing the coating detachment, which limits the functionality of the protective polymer.

The application of a combination of macro and micro techniques to characterize the material performance, such as vibrational spectroscopy and electron microscopy, can determine the suitability of the methods used to study these knowledge-intensive material composites. On the other hand, it is the intention of this experimental work to determine the damage mechanisms involved and the relationship between manufacturing and thermal effects implying changes at the surface level leading to adherence failures between the steel substrate and the protective PET polymer.

MATERIALS AND METHODS

The ECCS plate is coated with a fine, 0.02-μm thick layer of chromium oxide and metallic chromium that protects the steel from the environment and at the same time serves as a substrate, facilitating the adherence of the PET polymer to the material (Table I).

TABLE I
Chemical Composition of the Alloying Elements of the ECCS Plate Participating in the Alloy Iron

	Chemical Composition (wt %)						
	%C	%Mn	%P	%S°	%Si	%Al	N(ppm)
ECCS	0.074	0.260	0.021	0.016	0.012	0.032	45

In this study, 90 coupons of PET-coated ECCS plates, half of them having flat walls and the other half having crippled walls, mechanically formed by pressure, and obtained from new containers, were prepared. 0.1 m immersion trials in an acetic-acetate medium at room temperature and at pH 3.85, representative of fish and shellfish foods, in an open system at 40, 60, and 80°C, were performed.

Later, some samples were submitted to a constant polarization electrochemical test at 10 mV for 30 min in an acetic-acetate medium of the same characteristics above mentioned.

For all the analyses performed during this research, the following devices were used: Kaiser Holospec f/1.8i spectrometer, spectrum range 100-3800 cm^{-1}, and spectral resolution of 4 cm^{-1}; CCD Andor DV420A-OE-130 detector; and He-Ne laser Melles-Griot 0.5-lhp-151 at 632′8 nm.

The tested samples were analyzed by vibrational spectroscopy to determine the occurrence of changes in the PET composition because of absorption of the electrolyte, and changes at the structural level, in the crystallinity of the polymer, signifying alterations in the functionality of the coating. The power on the samples was kept under 10 mW avoid thermal damage. Also, they were macroanalyzed perpendicular to the coating surface by means of a laser at 785 nm to minimize fluorescence.

In addition, cross sections of the samples were microanalzsed parallel to the coating by Raman at 633 nm. Spectra were obtained every 5 μm at different points starting from the PET surface until reaching the ECCS interface.

In addition, an Fourier transform infrared spectroscopy-attenuated total reflection (FTIR-ATR) analysis with a 5-μm beam penetration to the PET coating was performed to evaluate the events occurring on the external surface, where the surface degradation of the coating starts. This technique is hypersensitive and was used to determine the interaction between the acetic-acetate electrolyte and the PET coating.

Furthermore, the samples were characterized by scanning electron microscopy (SEM) and chemically microanalyzed by X-ray dispersive energy, using a LEO 400 microscope and an Inca microprobe, respectively. The microanalysis implied graphite carbon shadowing to the PET coating to make the samples conductive. The former allowed to characterize and to determine the morphological changes of the material at a surface level caused by the manufacturing conditions, the thermal effect, and the action exerted by the acetic-acetate medium.

RESULTS AND DISCUSSION

Figure 1 shows the Raman spectra of a PET-coated ECCS plate sample taken perpendicular to the

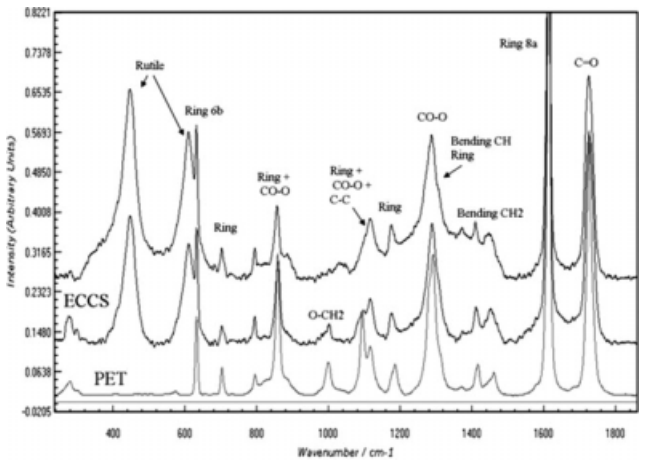

Figure 1 Interpretation of the material substrates by Raman spectroscopy.

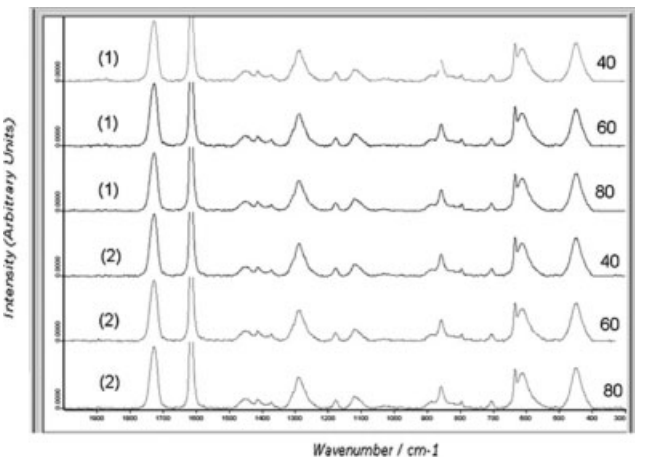

Figure 2 Comparison of Raman spectra for the flat (1) and rippled (2) wall coupons at different temperatures in an acetic-acetate medium.

surface and compared with the Raman spectrum of a pure PET sample. It is clear from these spectra that the coating contains rutile used as a filler of PET. Interpretation of the main vibrational bands is also included in this figure.

The micro-Raman measurements recorded the spectra across the complete surface of the flat and rippled wall coupons submitted to the different heating temperatures (40, 60, and 80°C) in the acetic-acetate medium. The spectra, showed no variations in the chemical composition due to an eventual interaction between the electrolyte and the polymer coating; that is, the measurements indicated that the PET was not affected in its composition by the electrolyte activity (Fig. 2).

Nevertheless a close-up analysis of the spectra obtained allowed the determination of small differences for the bands in the 900–1200 cm^{-1} spectral region associated with PET crystallinity and chain orientation.

The analyses of the flat wall samples, submitted to electrochemical polarization, after the micro-Raman spectroscopy evaluations at 40, 60, and 80°C, showed that those in the 80°C thermal treatment appeared less crystalline than those submitted to 40 and 60°C (Fig. 3).

The micro-Raman analyses of the rippled-wall mechanically deformed samples, under the same conditions of the previous trials, and submitted to the three temperatures, showed no evident spectral differences in this region, indicating no chemical interaction with the electrolyte (Fig. 4).

A detailed computer band profile analysis in this spectral region was performed to compare Raman

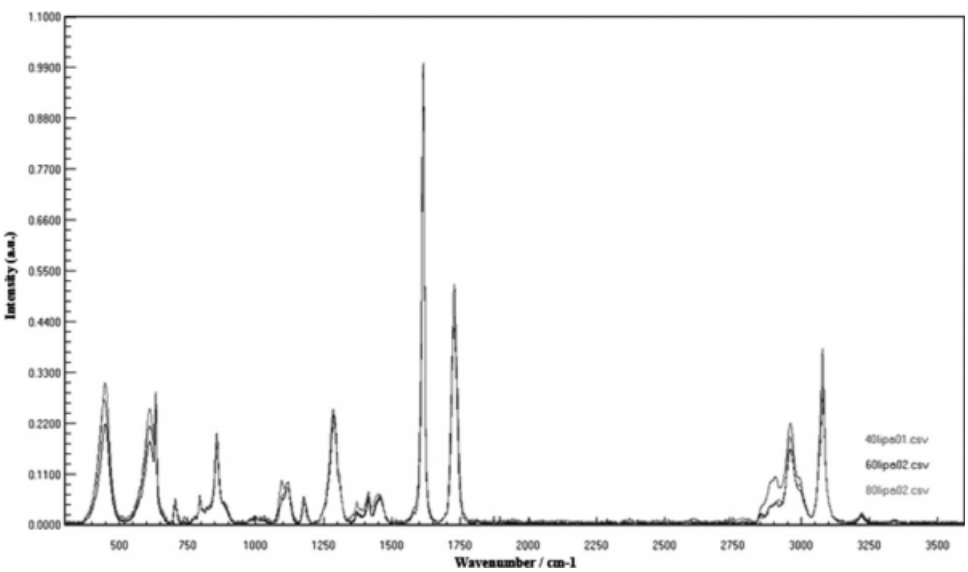

Figure 3 Comparison of flat samples submitted to electrochemical polarization at 40, 60, and 80°C (Micro-Raman).

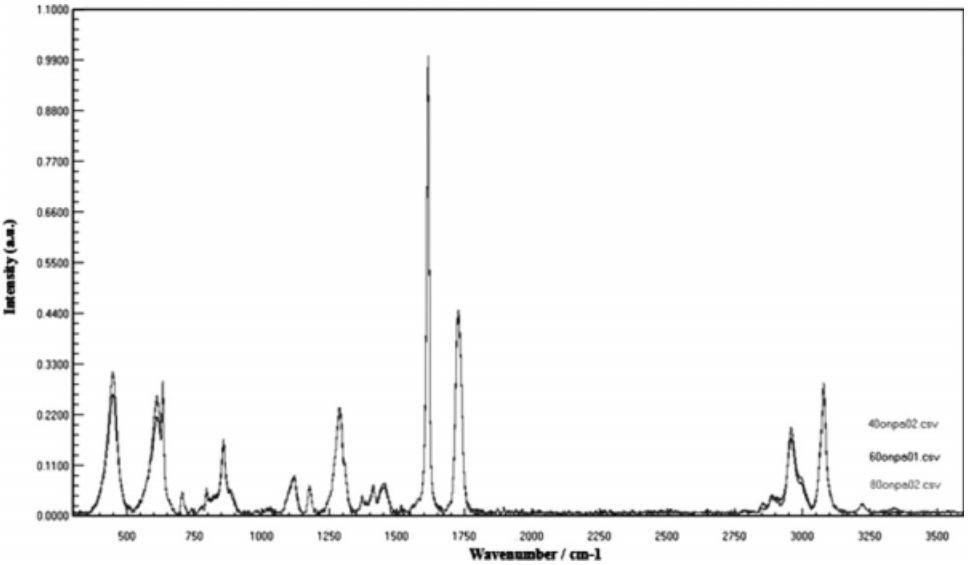

Figure 4 Comparison of rippled samples submitted to electrochemical polarization at 40, 60, and 80°C (Micro-Raman).

spectra of both flat and rippled samples. At each temperature the C—C + ν(C—C) ring band at 1096 cm^{-1}, corresponding to the chain vibrations associated with the crystalline region of the polymer, appeared weaker in the rippled samples when compared with the flat samples (Fig. 5). Therefore, the former variations associated to the rippled wall samples indicate that they were more amorphous than the more crystalline flat samples.

This implies that the changes detected were not the resulting action of the tested electrolyte but rather a consequence of the manufacturing process, which was validated by the measurements both by Raman and micro-Raman.

Complementary information on the effect of the acetic-acetate medium at different temperatures on the PET coating surface was obtained by FTIR-ATR analyses. Chemical and structural surface effects were easily observed because of the low depth of penetration of ATR into the analyzed samples, which is in the order of a few microns. The results of these analyses showed no variations in the vibrational bands of the PET, demonstrating that the surface was not attacked by the acid after the exposure time and temperatures applied. These results also validated and supported the Raman measurements, which indicated the absence of absorption of the chemical medium tested (Fig. 6).

In addition, micro-Raman analyses were performed in a geometrical configuration by striking the laser beam parallel to the coating deposit. The

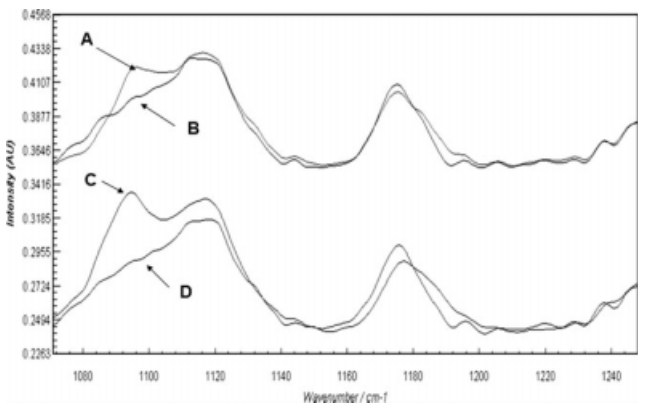

Figure 5 Micro-Raman spectral comparison between flat and rippled samples in the 1000-1200 cm^{-1} spectral range. A, flat sample at 80°C; B, rippled sample at 80°C; C, flat sample at 40°C; and D, rippled sample at 40°C.

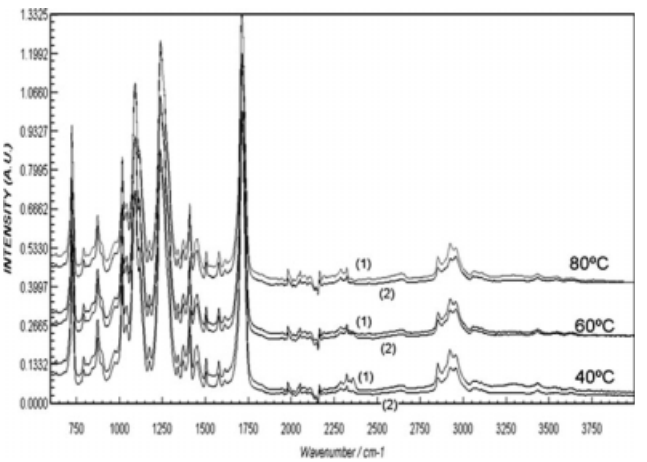

Figure 6 FTIR-ATR analysis of intensity variations in rippled wall sample at 80°C, performed at different points from the metallic interface through the external PET surface.

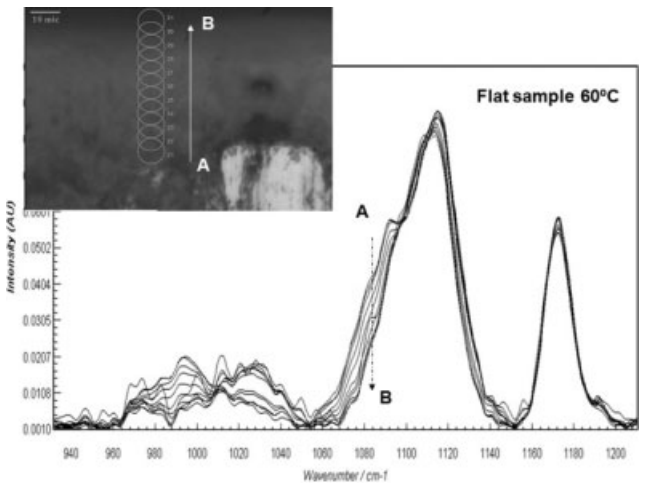

Figure 7 Micro-Raman spectra taken across the PET coating thickness at 5-μm intervals starting from the inner surface in contact with the metal.

PET coating was mapped taking spectra across its thickness in 5 μm steps starting at the metal-PET interface. Figure 7 show the results obtained with the flat samples exposed to the acid at 60°C. In contrast, the PET polymer coated control sample provides a clear vision of the changes undergone during the experimental conditions of the present work, and shows the profile of spectrum intensities associated to its chemical structure obtained after the bonding between the dimethylteraphthalate and ethylene glycol (Fig. 8).

A small decrease in crystallinity was observed when analyzing the span from the internal surface in contact with the metal to the external coating surface. However, no appreciable variation was observed in the rippled samples at the different temperatures. Therefore, the spectrum differences between flat and rippled coatings can also be associated to the manufacturing process rather to the interaction with the acid media. In this sense, the results obtained after surface microanalyses of

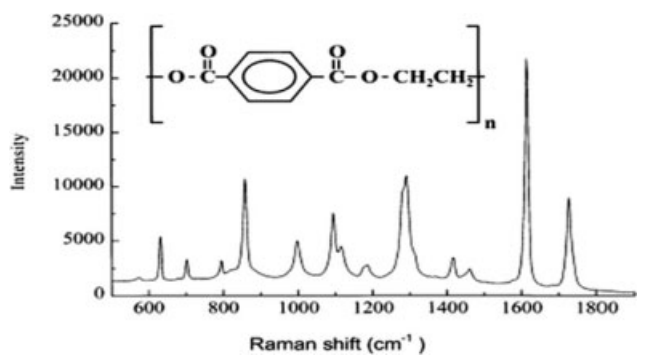

Figure 8 Raman spectrum of PET associated with its chemical structure.

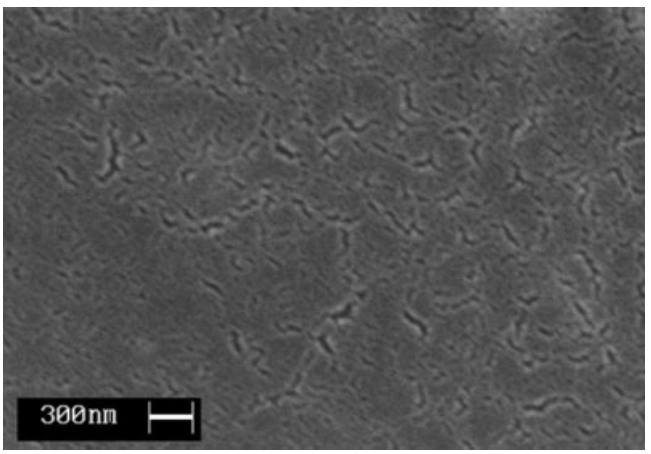

Figure 9 Morphology of PET coating on ECCS plate, mostly free of defects (SEM).

the tested samples at 785 nm to determine PET composition changes and changes in the polymer crystallinity were comparable with those obtained at 632.8 nm.

In general, the electron microscopy characterization established the existence of localized degradation on the protective coating, which was highly dependent on surface defects such as pores, scratches, deformations, detachments, etc. These defects regularly become the source of failures on the polymer substrate and lead to greater deterioration by the acetic-acetate medium however not compromising the entire functionality of the protective coating. Also, it must be mentioned that during this study these reduced localized defects were insufficient to allow the acid absorption, which facilitates the coating degradation, as demonstrated by the Raman vibrational spectroscopy analyses.

Figure 9 shows the PET coating with a continuous and semicrystalline spherulite-type surface morphology structure, which is associated to a good abrasion and corrosion resistance against aggressive food environments. The adherence capacity to the ECCS plate is located at the interface level, and as expected the PET coating shows an amorphous structure on that side.

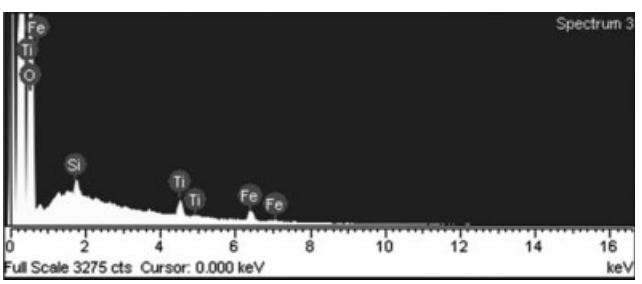

Figure 10 EDAX chemical analysis of PET coating.

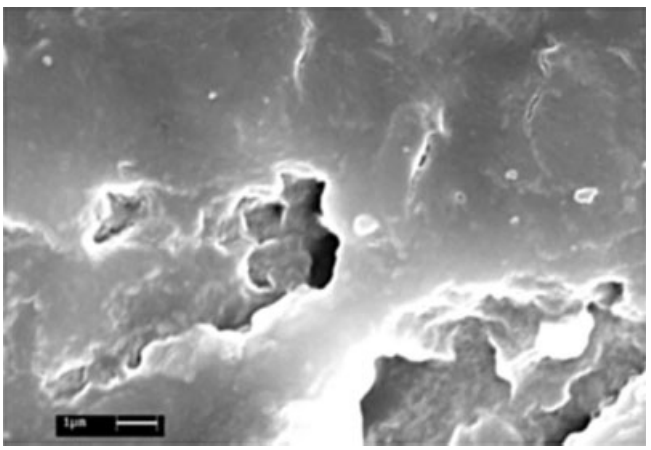

Figure 11 Flat sample tested at 40°C, showing a surface pore occurring during the PET manufacturing (SEM).

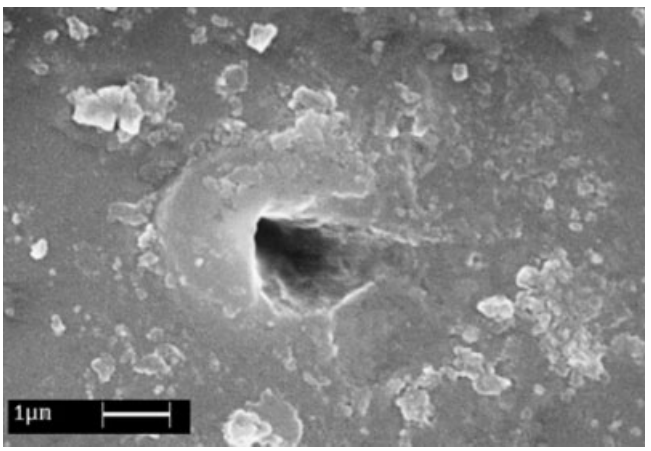

Figure 13 Flat sample tested at 80°C, exhibiting surface pore further degraded by acetic-acetate medium (SEM).

The X-ray dispersive analysis of the PET coating showed the non homogeneous presence of steel iron, the existence of silica in some multilayers under the PET, and detected the occurrence of rutile (TiO_2), which provides the polymer with its color and a photocatalyst effect for its protection by light to avoid the generation of cracks on its external surface (Fig. 10).

Figures 11, 12, and 13 give a view of the morphology observed in rippled samples, tested in the acid medium, and submitted to electrochemical polarization tests at different temperatures, and indicate the different distinctive localized deteriorations on the PET coating.

Coupons tested at 40°C in the acetic-acetated medium are representative of rippled samples, showing evident characteristic localized defects on the protective coating of steel (Figs. 14 and 15).

The former localized defects were a consequence of PET detachment from the ECCS plate, which normally promotes microcorrosion of the steel and limits its useful life, a factor that becomes critical when applying these materials in the manufacturing of food cans and containers.

Therefore, the need to obtain high quality manufacturing processes is a key element to achieve good mechanical and chemical adherence of the substrates, and a continuous and permeable PET surface free of pores and defects, to control the action of the electrolytic medium to avoid material degradation.

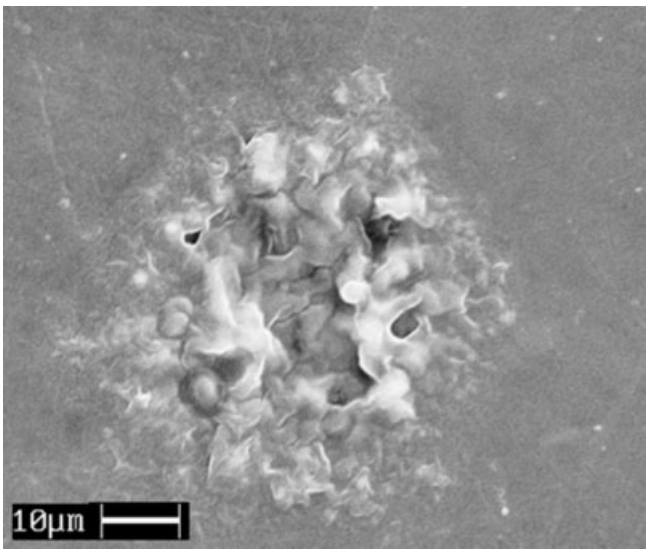

Figure 12 Flat sample tested at 60°C, indicating surface detachment defect caused by thermal shock action (SEM).

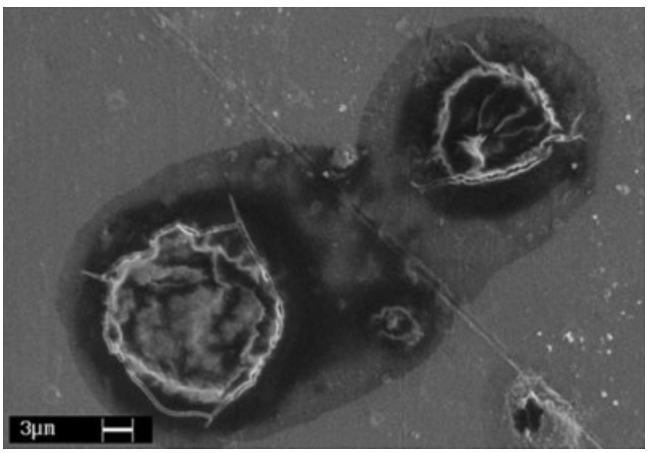

Figure 14 Rippled sample tested at 40°C, showing globular microdetachment of PET coating interacting with the acetic-acetate medium and directing to an increase in its volume and localized surface propagation (SEM).

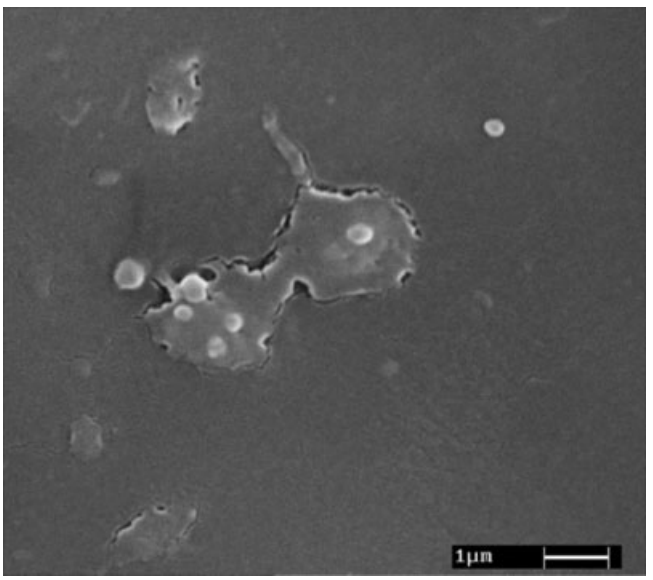

Figure 15 Rippled sample at 40°C heating exposure, exhibiting circular crack on the polymer surface resulting from manufacturing, which increased in size as an effect of the solution used (SEM).

CONCLUSIONS

From the present work, under the experimental conditions of study and considering the techniques applied, the following conclusions can be drawn:

1. The temperature had no effect on the acid absorption by the PET coating of samples tested in an acetic-acetate medium, a fact confirmed by the non significant spectral changes of the Raman and FTIR-ATR spectroscopies, indicating no changes in composition neither chemical realignments inducing to variations in the properties and functionalities of the polymer coating.
2. The Raman spectra showed that the flat, PET-coated ECCS plate samples evidenced greater crystallinity when compared with the rippled samples, being the latter more amorphous, which is explained by the mechanical deformation occurring during the manufacturing process to produce food containers. This deformation affects the material distinctly, since the polymer and the steel have different modules of elasticity.
3. The small spectral variations detected by micro-Raman in a parallel plane to the coating thickness, and which were manifest as an increase in crystallinity in the polymer from the external surface coating toward the metallic interface were a consequence of the mechanical deformation of containers where a combination of strong pressures and blows take place during the mechanical deep-drawing processing of materials, as confirmed by the characteristics of the control samples.
4. A particular effect on the PET surface, and focused on the manufacturing defects, was caused by the acetic-acetate medium, which increased the coating failures and induced deterioration spreading; however, without compromising the steel plate. The above situation leads to localized detachment points that limit the useful life of the composite in time.
5. The combination of micro- and macro-Raman techniques, electron microscopy, and electrochemical polarization allow to obtain convergent results in the characterization and evaluation of the protective capacity of PET's on ECCS plates.

References

1. Zumelzu, E.; Rull, F. Sci Eng Compos Mater 2002, 10, 71.
2. van der Aa, M. A. H.; Schreurs, P. J. G.; Baaijers, F. P. T. Mech Mater 2001, 33, 555.
3. Schrauwen, B. A. G.; Janssen, R.; Govaert, L.; Meijer, H. E. H. Macromolecules 2004, 37, 6069.
4. Cole, K. C.; Aijis, A.; Pellerin, E. Macromolecules 2002, 35, 770.
5. Rastogi, R.; Wellinga, W. P.; Rastogi, S.; Schick, C.; Meijer, M. E. H. J Polym Sci Part B: Polym Phys 2004, 42, 2092.
6. Zumelzu, E.; Cabezas, C.; Delgado, F. J Mater Process Technol 2004, 152, 384.
7. Zumelzu, E.; Rull, F.; Schmidt, P.; Boettcher, A. Surf Coat Int B 2006, 89, 57.
8. Hu, Y. S.; Liu, R. Y. F.; Zhang, L. Q.; Rogunova, M.; Shiraldi, D. A.; Nazarenko, S.; Hiltner, A.; Baer, E. Macromolecules 2002, 352, 7326.
9. Schick, C.; Wurn, A.; Mohammed, A. Termochim Acta 2003, 396, 119.
10. Wunderlich, B. Prog Polym Sci 2003, 28, 383.
11. Zumelzu, E.; Rull, F.; Boettcher, A. A. Surf Eng 2006, 7, 432.